Nano World Journal

http://dx.doi.org/10.17756/nwj.2016-028

Research Article

Open Access

Dielectric Response of $Ni_x Zn_{1-x} Al Fe O_4$ Nanoferrites

Paramesh Donta[1], Vijaya Kumar Katrapally[2*] and Venkat Reddy Pendyala[1]

[1]Sreenidhi Institute of Science and Technology (Autonomous), Ghatkesar, Hyderabad - 501301, Telangana, India

[2]Department of Physics, Jawaharlal Nehru Technological University Hyderabad College of Engineering Jagtial, Nachupally (Kondagattu), Karimnagar - 505501, Telangana, India

[*]Correspondence to:
Dr. K. Vijaya Kumar
Department of Physics, Jawaharlal Nehru Technological University Hyderabad College of Engineering Jagtial, Nachupally (Kondagattu)
Karimnagar - 505501, Telangana, India
E-mail: kvkphd@gmail.com

Received: July 16, 2016
Accepted: October 10, 2016
Published: October 12, 2016

Citation: Donta P, Katrapally VK, Pendyala VR. 2016. Dielectric Response of $Ni_x Zn_{1-x}$ Al Fe O_4 Nanoferrites. *NanoWorld J* 2(2): 27-34.

Published by United Scientific Group

Abstract

Ni-Zn-Al nanoferrites of general formula $Ni_x Zn_{1-x}$ Al Fe O_4 (x = 0.0, 0.2, 0.4, 0.6, 0.8 and 1.0) were synthesized by sol-gel auto combustion technique. The X-ray diffraction and FTIR studies confirmed the formation of single cubic spinel structure. Dielectric performance and AC conductivity of prepared mixed nanoferrites were carried out using LCR impedance meter. It was observed that both dielectric constant and dielectric loss were decreased by increasing the frequency whereas AC conductivity increases with applied frequency but decreases with increasing the Ni^{2+} ion substitution for a fixed Al^{3+} ion concentration. DC resistivity, activation energy and Curie temperature were calculated by using the two probe experimental method. It was observed that DC resistivity decreased whereas the charge mobility increased with increasing the temperature. DC resistivity and activation energy of the nanoferrite samples were increased with Ni^{2+} ion substitution for a fixed Al^{3+} ion concentration.

Keywords

Ni-Zn-Al nanoferrites, Spinel structure, Dielectric constant, Dielectric loss, AC conductivity, DC resistivity

Introduction

Investigating the properties of nanoferrites is the most important in the fast growing areas like scientific, industries, design and research of nano technology. Ni–Zn ferrite is a soft magnetic and an important ceramic material which has enormous applications in various fields like electric, magnetic, electronics, microwave devices, catalysts, transformers cores, power conversions, high frequency applications in telecommunications, magnetically control drug delivery system, for multilayer inductor applications, etc [1-7]. The nanoferrite properties can be easily adjustable, controllable to a great extent by choosing proper preparation methods and suitable doping with divalent, trivalent and rare earth ions [8-10]. Different cation substitutions can distribute into the voids of the parent crystal structure and can alter many properties of nanoferrites like DC resistivity, mobility of the charge, desire magnetization, activation energy, Curie temperature and dielectric losses. Electrical conductivity gives the significant information about conduction mechanism of ferrites. The electric conductivity of ferrites depends on various parameters like preparation methods, type of doping, temperature and sintering conditions and time [11,12]. Impedance spectroscopy is an outstanding technique to analyze the electrical conduction mechanism of ferrites. The AC conductivity of the ferrites can be investigated in many ways like complex impedance, complex permittivity

and complex electric modulus [13]. But all are equally valid to study the electrical conduction mechanism of ferrites.

The purpose of this work is to synthesis the $Ni_x Zn_{1-x} Al Fe O_4$ (x = 0.0, 0.2, 0.4, 0.6, 0.8 and 1.0) nanoferrites and to understand the influence of Ni^{2+} ion substitution for a fixed Al^{3+} ion concentration on the structural, magnetic, dielectric and electrical properties of Ni-Zn nanoferrites. In this article, we have been focused mainly on the dielectric behaviour and DC electrical resistivity of all the prepared nanoferrites. The study of dielectric constant, dielectric loss and AC conductivity is made as a function of frequency and composition at room temperature. In addition to this the study of dielectric loss, AC conductivity and DC resistivity is made as a function of temperature. The DC electrical resistivity of all the samples were found in the order of 10^6 [14] and low dielectric loss values was found, hence these ferrites may be suitable for making high frequency electronic devices and electromagnetic wave absorbing devices.

Experimental

Synthesis route

Analytical grade (AR) with 99% purity of chemical reagents such as zinc nitrate hexahydrate – $Zn(NO3)_2 6H_2O$ (AR), nickel nitrate – $Ni(NO3)_2 6H_2O$ (AR), aluminium nitrate nonahydrate – $Al(NO3)_3 9H_2O$ (GR), ferric nitrate – $Fe(NO3)_3 9H_2O$ (GR) & citric acid monohydrade – $C_6 H_8 O_7 H_2O$ (GR) were used for the preparation of aluminium substituted Ni-Zn nanoferrites of general formula $Ni_x Zn_{1-x} Al Fe O_4$ (x = 0.0, 0.2, 0.4, 0.6, 0.8 and 1.0) using sol-gel auto combustion technique. Stoichiometric chemical reagents were dissolved in de-ionized water. Mixed nitrate solution was magnetically stirred for an hour then citric acid was added to nitrate solution in 3:1 molar ratio and further stirred for half an hour at 60 °C temperature. Liquid ammonia was added to citric solution to maintain P^H value at 7.0 and by continuously stirring on the hot plate at 100 °C to get a viscous gel. The gel was kept on heating till it burns and undergoes combustion. As a result of auto-combustion finally fluffy powder of synthesized ferrite was obtained. The fine powder was calcined under the constant heating conditions at 873 K for 5 hours and grinded into fine particles. Finally, the calcined fine powder was pressed into pellets of 10 mm diameter and approximately 1-2 mm thickness.

The pellets were calcined at 873 K for 5 hours for further investigations. Both surfaces of the pellet samples were coated with silver paste for better electrical contact to study its electrical properties. Using pellet samples, the dielectric behaviour and AC conductivity were carried out by LCR impedance meter (Model 6500P Precision LCR Meter, Wayne Kerr, Germany) as a function of frequency (20 Hz – 5 MHz) and the temperature (room temperature to 873 K). DC resistivity of ferrite samples was carried out by using two probe experimental set-ups (Model DNM-121, SES Instruments Pvt. Ltd, Roorkee, India).

Results and Discussions

X-ray diffraction study

The structural analysis of $Ni_x Zn_{1-x} Al Fe O_4$ (x = 0.0, 0.2, 0.4, 0.6, 0.8 and 1.0) ferrite nanoparticles was studied by powder XRD method using CuK_α radiation. Figure 1 shows the X-ray diffraction patterns of all prepared ferrite nanoparticles which confirmed the crystalline structure. The average crystallite size (t) of the ferrite nanoparticles were calculated using the Debye-Scherrer formula (Eq.1) and was found in the range 15-46 nm.

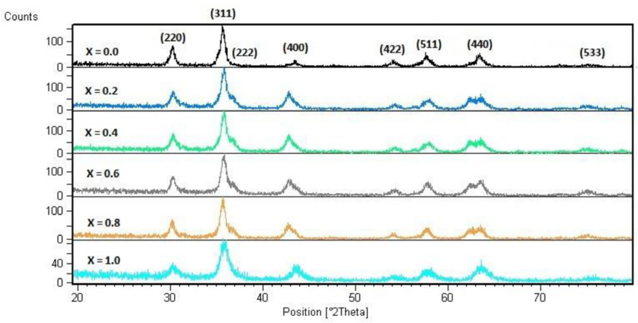

Figure 1: X-ray diffraction pattern of $Ni_x Zn_{1-x} Al FeO_4$(x = 0.0, 0.2, 0.4, 0.6, 0.8 and 1.0).

$$t = \frac{0.9\lambda}{\beta\cos\theta} \quad \ldots\ldots\ldots\ldots\ldots\ldots (1)$$

Where, λ – Wavelength of the X-ray radiation, β – full width at half maximum, θ – Bragg's angle.

The lattice constant was determined by Eq.(2)

$$a = d\sqrt{h^2 + k^2 + l^2} \quad \ldots\ldots\ldots\ldots\ldots\ldots (2)$$

Where, d – inter planer distance, h, k, l – Miller indices.

It was noticed that the crystallite size and lattice constant values gradually decreased with increasing of Ni^{2+} ion substitution. Decrease in the crystallite size and lattice constant may be due to the substitution of smaller Ni^{2+} ions (0.74 Å) in place of larger Zn^{2+} ions (0.84 Å) [15-18].

The X-ray density (ρ_X), bulk density (ρ_B) and porosity was calculated by Eq. (3), (4) and (5) respectively and listed in Table 1.

$$\rho_x = \frac{8M}{Na^3} \quad \ldots\ldots\ldots\ldots\ldots\ldots (3)$$

Where, M - molecular weight, N - Avogadro number, a - lattice constant.

$$\rho_B = \frac{m}{\Pi r^2 t} \quad \ldots\ldots\ldots\ldots\ldots\ldots (4)$$

Where, m - mass of the circular pellet, r – radius of the pellet, t – thickness of the pellet.

$$P = 1 - \frac{\rho_B}{\rho_X} \quad \text{..... (5)}$$

Where, P – porosity, ρ_B – bulk density, ρ_X – X-ray density.

From Table 1, it was observed that the X-ray density and porosity decreased, bulk density increased with increase of Ni^{2+} ion substitution for a fixed Al^{3+} ion concentration. In the case of ferrites, the X-ray density is more than the bulk density. It is due to existence of pores in the samples, which depend on sintering temperature. The X-ray density depends on the molecular weights of the samples and lattice constants. The molecular weights of prepared samples of $Ni_x Zn_{1-x} Al Fe O_4$ (x = 0.0, 0.2, 0.4, 0.6, 0.8 and 1.0) were found to decrease from 212.15 to 205.46 g/mol by varying the composition (x). Hence, the X-ray density decreased as Ni^{2+} ion substitution increased [19]. The bulk density and porosity was inversely related with each other. Hence, the bulk density increased and the porosity progressively decreased with the increase of Ni^{2+} ion substitution (Table 1). It confirms densification of the samples as the Ni^{2+} ion substitution is increased for a fixed Al^{3+} ion concentration [20].

Table 1: Lattice constant (a), X-ray density (ρ_x), Bulk density (ρ_B), Porosity (P) and crystallite size (t) of $Ni_x Zn_{1-x} Al FeO_4$ (x = 0.0, 0.2, 0.4, 0.6, 0.8 and 1.0).

Composition (x)	Lattice constant (a) (Å)	X-ray density(ρ_x) (gm/cm^3)	Bulk density (ρ_B) (gm/cm^3)	Porosity (P) (%)	Crystallite size (t) (Debye-Scherer) (nm)
0.0	8.334	4.869	3.784	22.28	45.74
0.2	8.327	4.850	3.893	20.22	45.74
0.4	8.314	4.842	3.905	19.35	41.16
0.6	8.307	4.824	3.947	18.18	34.29
0.8	8.295	4.814	3.981	17.30	20.58
1.0	8.281	4.807	3.997	16.85	14.70

FTIR study

The FTIR spectra of $Ni_x Zn_{1-x} Al Fe O_4$ (x = 0.0, 0.2, 0.4, 0.6, 0.8 and 1.0) were taken in the range 350 - 750 cm^{-1} at room temperature which is annealed at 873 K shown in Figure 2. The FTIR spectra confirmed the formation of spinel cubic structure and the strong absorption bands with two characteristic peaks [21-24]. In ferrites the metal ions are situated at two sub-lattices named tetrahedral (A) site and octahedral (B) site. The high frequency tetrahedral (υ_1) band was observed in the range of 605-636 cm^{-1} and low frequency octahedral band (υ_2) was observed in the range of 404-414 cm^{-1} and shown in Table 2. This confirms the spinel structure of the prepared ferrite compositions. Similar reports were observed by Zahi and Pathak [25, 26].

Dielectric response

Impedance spectroscopy is a common technique to study the property of electrical conduction of ceramic materials in terms of dielectric response as a function of AC field. Dielectric properties of nanoferrites were affected by the applied temperature, frequency of AC field and its lattice structure. Dielectric behaviour of a ferrite material under alternating electric fields can be explained as complex permittivity ($\varepsilon^* = \varepsilon' + j\varepsilon''$). Complex permittivity of the dielectric material depends on several parameters such as microstructure, oxygen vacancy, cation substitutions, preparation methods and sintering temperature.

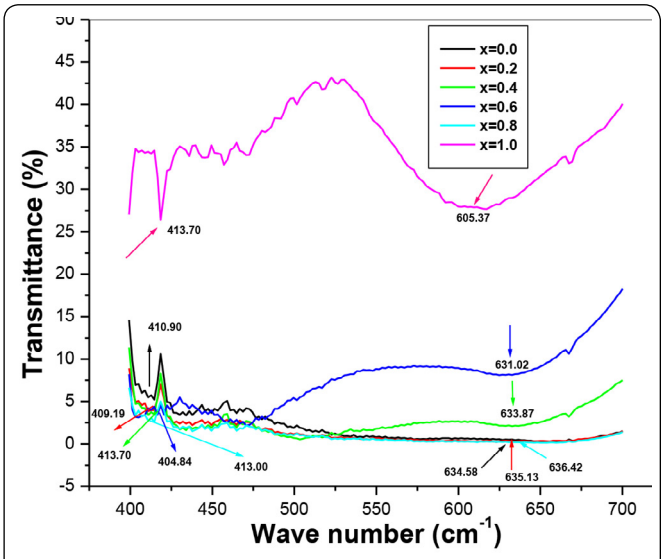

Figure 2: FTIR image of $Ni_x Zn_{1-x} Al FeO_4$ (x = 0.0, 0.2, 0.4, 0.6, 0.8 and 1.0).

Table 2: Tetrahedral and Octahedral frequencies of $Ni_x Zn_{1-x} AlFeO_4$ (x = 0.0, 0.2, 0.4, 0.6, 0.8 and 1.0).

Composition (x)	Tetrahedral frequencies (υ_1) (cm^{-1})	Octahedral frequencies (υ_2)(cm^{-1})
0.0	634	411
0.2	635	409
0.4	634	414
0.6	631	404
0.8	636	413
1.0	605	414

Complex dielectric permittivity was calculated with Eq. (6),

$$\varepsilon^* = \varepsilon' + j\varepsilon'' \quad \text{..... (6)}$$

Real and imaginary parts of permittivity can be calculated by Eqs. (7) and (8) respectively.

$$\varepsilon' = \frac{Cd}{\varepsilon_0 A} \quad \text{..... (7)}$$

$$\varepsilon'' = \varepsilon' \tan \delta \quad \text{..... (8)}$$

Where, ε' – real part permittivity, ε" – imaginary part permittivity, C – capacitance, d – thickness of the pellet, A – surface area of the pellet, ε_0 – permittivity of free space, tan δ – dielectric loss factor.

Figure 3 (A) and (B) shows the dielectric behaviour of real and imaginary parts of complex dielectric permittivity with applied frequency (20-1 MHz) of $Ni_x Zn_{1-x}$ Al Fe O_4 (x = 0.0, 0.2, 0.4, 0.6, 0.8 and 1.0) nanoferrites at room temperature (304 K). It was found that the real and imaginary parts of dielectric permittivity decreased with increasing the applied frequency which shows the dielectric dispersion at lower frequency. This dispersion mechanism at low frequency was explained by the Maxwell-Wagner's two-layer model [27-30] in agreement with Koop's phenomenological theory [31]. The changing in the dielectric constant maybe explained in terms of space charge polarization which is produced due to the existence of greater conductivity grains in the insulating grain boundaries [32-37]. The space charge polarization is formed due to large fine conducting grains separated by thin poor conducting intermediate grain boundaries.

The exchange of electron between Fe^{2+} and Fe^{3+} ions gives the local displacement of electrons in the applied AC field direction which gives the polarization. It was found that the polarization decreases with increased frequency and gets a stable value at a particular higher frequency. This can be explained that beyond a certain applied frequency the electron exchange between $Fe^{2+} \leftrightarrow Fe^{3+}$ does not follow the AC field.

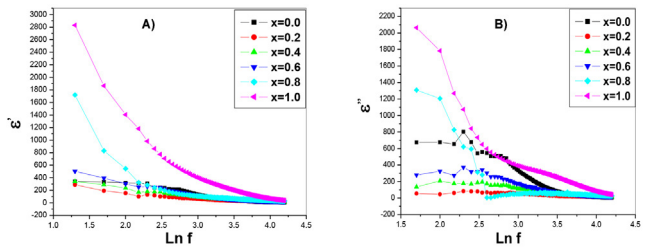

Figure 3: Variation of **(A)** Real part permittivity with frequency **(B)** imaginary part permittivity with frequency of $Ni_x Zn_{1-x}$ Al FeO_4 (x = 0.0, 0.2, 0.4, 0.6, 0.8 and 1.0) at room temperature.

AC Conductivity

Figure 4 illustrates the variation of AC conductivity with applied frequency at room temperature as function of Ni^{2+} ion substitution for a fixed Al^{3+} ion concentration. AC conductivity of the ferrite samples was calculated by Eq. (9).

$$\sigma_{AC} = \omega \varepsilon_0 \varepsilon'' \quad \ldots\ldots\ldots\ldots\ldots\ldots\ldots\ldots\ldots\ldots (9)$$

Where, ω – Angular frequency

Usually the electrical conductivity in ferrites may explain on the basis of Verwey conduction mechanism, where the electron exchange takes place between the adjacent Fe^{2+} and Fe^{3+} ions which occupied the octahedral sites [38]. From Figure 4, it was found that the AC conductivity increased linearly with frequency of applied field, this shows the general behaviour of ferrite structures. The linear increase in electrical conductivity by increasing the applied frequency can be explained as the increasing frequency can improve the electron hopping between the charge carriers and thus increasing the electric conductivity of the nano ferrites [39, 40].

It was observed from Figure 4 that AC conductivity decreases with increasing the Ni^{2+} ion substitution for a fixed Al^{3+} ion concentration. This can be explained by microstructure, jump length and the jumping probability of electrons. It was found that the crystallite size decreased from 45.74 to 14.70 nm with increasing the Ni^{2+} ion substitution which is shown in Table 1. Hence it is clear that lesser the grain size larger will be the insulating grain boundaries and less will be the electrical conductivity of the material. As grains and particle size is decreasing with increasing the Ni^{2+} ion substitution for a fixed Al^{3+} ion concentration consequently AC conductivity decreases linearly which shows small polarons are responsible for conduction mechanism [41]. In another way it may be explained that the smaller grains offer a large number of insulating grain boundaries which are acting as a barrier for the electric current hence there is a reduction in the electric current of the ferrite material [42]. The dielectric parameters of $Ni_x Zn_{1-x}$ Al Fe O_4 (x = 0.0, 0.2, 0.4, 0.6, 0.8 and 1.0) nanoferrites at room temperature were tabulated in Table 3.

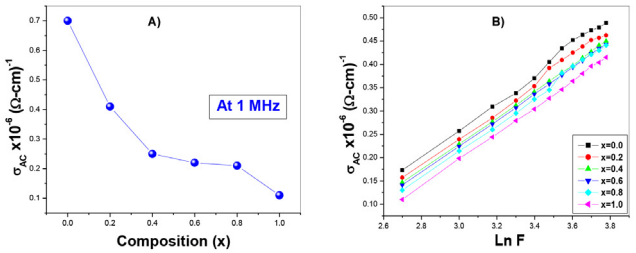

Figure 4: Variation of **(A)** AC conductivity with composition **(B)** AC conductivity with frequency of $Ni_x Zn_{1-x}$ Al FeO_4 (x = 0.0, 0.2, 0.4, 0.6, 0.8 and 1.0) at room temperature.

Table 3: Dielectric constant (ε'), dielectric loss (tan δ), A.C conductivity (σ_{AC}) of $Ni_x Zn_{1-x}$ $AlFeO_4$ (x = 0.0, 0.2, 0.4, 0.6, 0.8 and 1.0) at room temperature.

Composition (x)	Dielectric constant (ε') at 1 MHz	Dielectric loss (tan δ) at 1 MHz	A.C conductivity (σ_{AC}) $(\Omega\text{-cm})^{-1}$
0.0	92.25	1.06	0.70×10^{-6}
0.2	43.87	0.93	0.41×10^{-6}
0.4	33.02	0.91	0.25×10^{-6}
0.6	26.04	0.88	0.22×10^{-6}
0.8	21.17	0.86	0.21×10^{-6}
1.0	19.60	0.82	0.11×10^{-6}

Temperature dependent AC Conductivity

The temperature dependence of dielectric loss tangent (tan δ), AC conductivity (σ_{AC}) of the samples at the composition of x = 0.4, 0.8 and 1.0 were shown in Figure 5 & 6 respectively. It was found that the AC conductivity and dielectric loss tangent were increased with increasing the temperature which confirming the semiconducting behaviour of ferrite material [43].

This shows there is a strong association between the conduction mechanism and the dielectric behaviour of ferrites [44, 45]. It can be observed that by increasing the temperature

the electrical conductivity and dielectric loss tangent of ferrite samples were increased. This is due to increase in temperature which can thermally activate the charge carriers that in turn increases the charge exchange interactions. Hence the AC conductivity and dielectric loss tangent were increased with temperature. The dielectric parameters of $Ni_x Zn_{1-x}$ Al Fe O_4 (x = 0.0, 0.2, 0.4, 0.6, 0.8 and 1.0) nanoferrites at room temperature were tabulated in Table 3.

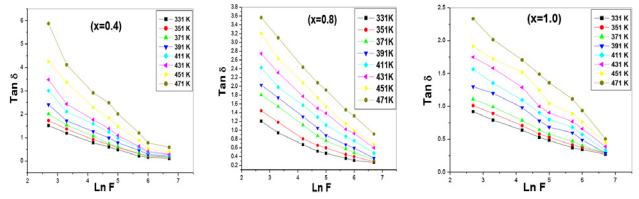

Figure 5: Variation of dielectric loss tangent with frequency of $Ni_x Zn_{1-x}$ Al FeO_4 (x = 0.4, 0.8 and 1.0) at different temperatures.

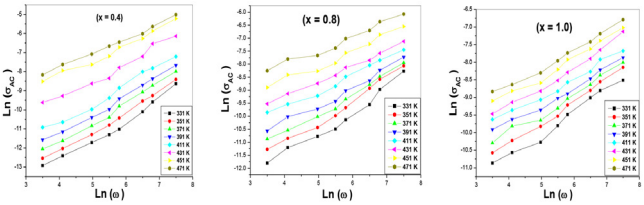

Figure 6: Variation of AC conductivity with frequency of Nix Zn1-x Al Fe O4 (x = 0.4, 0.8 and 1.0) at different temperatures.

DC Electrical Resistivity

The DC electrical resistivity of the ferrite materials was decided by the chemical composition, type of materials used, preparation method, sintering temperature, crystallite size, density, porosity, crystallography of the samples and type of cations substitutions in the ferrite lattice [46]. Ferrite electrical resistivity may alter by substitution of suitable divalent or trivalent ions occupying into the tetrahedral or octahedral sites. The present work talks the influence on DC resistivity with Ni^{2+} ion substitution for a fixed Al^{3+} ion concentration in Zn nanoferrite. The DC electrical resistivity of the ferrite samples was studied by applying the temperature within the range 294-873 K using two-probe experimental set-up.

Resistivity of the samples and drift mobility of the charge carriers were calculated using the Eq. (10), (11) and (12).

$$\rho = \frac{RA}{L} \quad \ldots\ldots\ldots\ldots\ldots\ldots\ldots\ldots\ldots\ldots (10)$$

Where, R - resistance, A - area of the sample, L - thickness of the pellet sample

$$\mu_d = \frac{1}{nep} \quad \ldots\ldots\ldots\ldots\ldots\ldots\ldots\ldots\ldots\ldots (11)$$

Where, e – electron charge, ρ – DC resistivity, n - charge concentration

$$n = \frac{N_A \rho_B P_{Fe}}{M} \quad \ldots\ldots\ldots\ldots\ldots\ldots\ldots\ldots\ldots\ldots (12)$$

Where, N_A – Avogadro number, ρ_B – bulk density, P_{Fe} – number of atoms, M – molecular weight

It was noticed that the electrical resistivity and drift mobility are inversely related, hence samples have high electrical resistivity shows low drift mobility and vice versa. Figure 7 (A) shows DC electrical resistivity with temperature (B) drift mobility of charges with temperature of $Ni_x Zn_{1-x}$ Al Fe O_4 (x = 0.0, 0.2, 0.4, 0.6, 0.8 and 1.0) nanoferrites. Figure 7 (A) and (B) shows that the temperature increased resistivity decreased and drift mobility increased which is indicating the semiconductor behaviour of the samples.

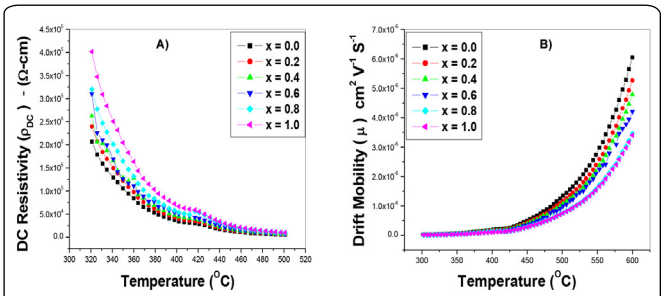

Figure 7: Variation of **(A)** DC resistivity with temperature **(B)** drift mobility with temperature of $Ni_x Zn_{1-x}$ Al FeO_4 (x = 0.0, 0.2, 0.4, 0.6, 0.8 and 1.0).

The variation of DC electrical resistivity of $Ni_x Zn_{1-x}$ Al Fe O_4 (x = 0.0, 0.2, 0.4, 0.6, 0.8 and 1.0) nanoferrites as a function of temperature and composition is shown in Figure 8. It was clear from Figure 8 that the electrical resistivity of ferrite samples found to decrease with increasing the temperature showing the semiconductor behaviour of ferrite samples. Decrease in the electrical resistivity by increasing temperature can be explained due to thermally activated drift mobility of charge carriers according to hopping conduction mechanism [47, 48] of electrons between multivalent cations like Fe^{2+} and Fe^{3+} located at octahedral sites as $Fe^{3+} + e^- \leftrightarrow Fe^{2+}$.

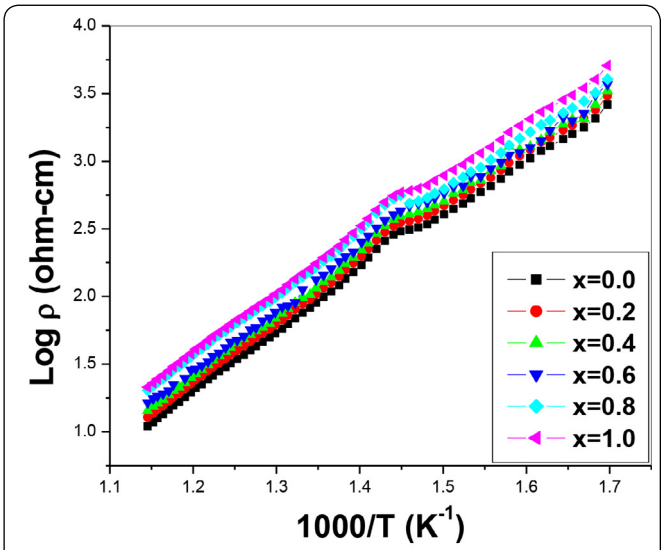

Figure 8: Variation of DC electrical resistivity with 1000/T of $Ni_x Zn_{1-x}$ Al FeO_4 (x = 0.0, 0.2, 0.4, 0.6, 0.8 and 1.0).

Sonal Singhal et at. observed that the resistivity increases with the decrease of Ni^{2+} ion concentration in the case of

Ni-Zn nano ferrites [19], where as in our Ni-Zn-Al nano ferrites, it has been found that the resistivity increases with the increase of Ni^{2+} ion substitution. And the order of resistivity is lower in case of Ni-Zn-Al nano ferrites than the Ni-Zn ferrites [19]. The lowering of resistivity could be understood due to substitution of Al^{3+} ions (having low third ionization energy, 2744 KJ/mol) in the place of Fe^{3+} ions (2951 KJ/mol). Hence the substitution of Al^{3+} ions playing significant role in determining the electrical properties.

It is clear from the Figure 8 that the DC resistivity of the ferrite samples slightly increases from 0.206 x 10^6 to 0.399 x 10^6 Ω-cm with increasing the Ni^{2+} ion substitution for a fixed Al^{3+} ion concentration shown in Table 4. The increase in electrical resistivity of the ferrite samples may be explained due to the preferential tendency nature of Ni^{2+} and Al^{3+} ions to occupy either tetrahedral sites or octahedral sites. But both Ni^{2+} and Al^{3+} ions prefer to occupy the octahedral sites [49, 50] hence increasing the Ni^{2+} ion substitution for a fixed Al^{3+} ion concentration may cause to shift the Fe^{3+} ions from octahedral sites to tetrahedral site. Therefore, it was observed that the decrease in electron transfer in between $Fe^{2+} \leftrightarrow Fe^{3+}$ consequently the resistivity of the sample increases with increasing the Ni^{2+} ion substitution for a fixed Al^{3+} ion concentration. The conduction process in Ni-Zn ferrites can also explain due to hopping of electrons from Fe^{2+} to Fe^{3+} ions and transfer of the charge by hole from Ni^{3+} to Ni^{2+} [51].

This can be explained by the following mechanism

$Ni^{2+} + Fe^{3+} \leftrightarrow Ni^{3+} + Fe^{2+}$

Table 4: Curie temperature, DC resistivity and activation energy of $Ni_x Zn_{1-x}$ Al Fe O_4 (x = 0.0, 0.2, 0.4, 0.6, 0.8 and 1.0).

Composition (x)	Curie T emperature (K)		DC resistivity at room temperature (Ω-cm)	E_P (eV)	E_F (eV)	ΔE (eV)
	Two probe method	Lorie-Sinha method				
0.0	671	678	0.206 x 10^6	0.706	0.483	0.223
0.2	668	672	0.237 x 10^6	0.716	0.487	0.229
0.4	664	667	0.260 x 10^6	0.727	0.489	0.232
0.6	658	662	0.307 x 10^6	0.736	0.498	0.238
0.8	653	654	0.320 x 10^6	0.747	0.504	0.243
1.0	647	643	0.399 x 10^6	0.763	0.513	0.250

Activation energy and Curie temperature

Figure 8 shows the Arrhenius plot of $Ni_x Zn_{1-x}$ Al Fe O_4 (x = 0.0, 0.2, 0.4, 0.6, 0.8 and 1.0) nanoferrite samples. The activation energy values were obtained from the slopes of ferrimagnetic (E_F) and paramagnetic regions (E_P) and they are posted in Table 4. It was found that the activation energy of paramagnetic region (E_P) is greater than that of ferrimagnetic region (E_F) for all ferrite samples. In ferromagnetic region the conduction electrons are very actively make hopping mechanism between Fe^{2+} and Fe^{3+} ions in B sites, which lower the value of activation energy [52]. From Table 4, it can be understood that the activation energy values increased from 0.223 to 0.250 eV with increasing the Ni^{2+} ion substitution for a fixed Al^{3+} ion concentration. This is due to the existence of a large number of oxygen vacancies and the increasing trend electrical resistivity of the ferrite samples.

In Figure 8, the kink at a particular temperature signifying that the ferrite samples transform from ferrimagnetism to paramagnetism and this temperature is known as Curie temperature. From Table 4 it was noticed that the Curie temperature decreased from 671 to 647 K with increase of Ni^{2+} ion substitution for a fixed Al^{3+} ion concentration. The Curie temperature values obtained from the Arrhenius plots and that of Lorie - Sinha method are found to be nearly equal.

Conclusion

We have successfully prepared nanoferrites having the formula of $Ni_x Zn_{1-x}$ Al Fe O_4 (x = 0.0, 0.2, 0.4, 0.6, 0.8 and 1.0) using the sol-gel auto combustion technique. XRD results reveal that all samples have single phase cubic spinel structure. Lattice parameters and crystallite size were found to decrease with Ni^{2+} ion substitution for a fixed Al^{3+} ion concentration. IR absorption spectra shows that the two fundamental bands ν_1 and ν_2 are in the frequency range 600 – 400 cm^{-1}. Frequency and temperature dependent dielectric response was studied in the frequency range 20-5 MHz and the temperature range 304 to 873 K respectively. It was found that at room temperature dielectric constant and dielectric loss tangent decreases with increasing the frequency and Ni^{2+} ion substitution for a fixed Al^{3+} ion concentration. It was noticed that the dielectric constant (19.60) and dielectric loss (0.82) values were minimum for composition x = 1.0 and both values are increased with increasing temperature. The low dielectric loss materials can be used in radio-frequency and microwave communications. The DC electrical resistivity of the ferrite samples found to decrease with increasing the temperature and it increases with increasing Ni^{2+} ion substitution for a fixed Al^{3+} ion concentration. The Curie temperature was decreased and activation energy increases with increasing the Ni^{2+} ion substitution for a fixed Al^{3+} ion concentration.

Acknowledgements

The authors DP and PVR are grateful to the Principal and Executive Director, SNIST, Ghatkesar, Hyderabad for their support. The author KVK is thankful to Prof. N.V. Ramana, Principal, JNTUH CE, Nachupally (Kondagattu), Karimnagar District, Telangana State-India, for his constant encouragement in bringing out this research work.

References

1. Spaldin NA, Fiebig M. 2005. The renaissance of magnetoelectric multiferroics. *Science* 309(5733): 391-392. doi: 10.1126/science.1113357
2. Fuller AJB.1987. Ferrites at microwave frequencies. Peter Peregrinus Ltd, London, United Kingdom.
3. How H. 1999. Magnetic microwave devices. In: Webster JG (eds) Wiley Encyclopedia of Electrical and Electronics Engineering, Wiley, New York, USA.
4. Singh N, Agarwal A, Sanghi S, Singh P. 2011. Synthesis, microstructure, dielectric and magnetic properties of Cu substituted Ni-Li ferrites. *J Magn Magn Mater* 323(5): 486-492. doi: 10.1016/j.jmmm.2010.09.053

5. Gabal MA, Al Angari YM. 2009. Effect of chromium ion substitution on the electromagnetic properties of nickel ferrite. *Mater Chem Phys* 118(1): 153-160. doi: 10.1016/j.matchemphys.2009.07.025

6. Sharma DR, Mathur R, Vadera SR, Kumar N, Kutty TRN. 2003. Synthesis of nanocomposites of Ni-Zn ferrite in aniline formaldehyde copolymer and studies on their pyrolysis products. *J Alloys Compd* 358(1-2): 193-204. doi: 10.1016/S0925-8388(03)00034-3

7. Kambale RC, Adhate NR, Chougle BK, Kolekar YD. 2010. Magnetic and dielectric properties of mixed spinel Ni-Zn ferrites synthesized by citrate-nitrate combustion method. *J Alloys Compd* 491(1-2): 372-377. doi: 10.1016/j.jallcom.2009.10.187

8. Shelar MB, Jadhav PA, Chougule SS, Mallapur MM, Chougule BK. 2009. Structural and electrical properties of nickel cadmium ferrites prepared. *J Alloys Compd* 476(1-2): 760-764. doi: 10.1016/j.jallcom.2008.09.107

9. Patange SM, Shirsath SE, Toksha BG, Jadhav SS, Jadhav KM. 2009. Electrical and magnetic properties of Cr^{3+} substituted nanocrystalline nickel ferrite. *J Appl Phys* 106(2): 023914. doi: 10.1063/1.3176504

10. Shinde TJ, Gadkari AB, Vasambekar PN. 2012. Influence of Nd^{3+} substitution on structural, electrical and magnetic properties of nonocrystalline nickel ferrites. *J Alloys Compd* 513: 80-85. doi: 10.1016/j.jallcom.2011.10.001

11. Shaikh AM, Kanamadi CM, Chougule BK. 2005. Electrical resistivity and thermoelectric power studies on Zn-substituted Li-Mg ferrites. *J Mater Chem B Mater Biol Med* 93(2-3): 548-551. doi: 10.1016/j.matchemphys.2005.04.005

12. Sivakumar N, Narayanasamy A, Greneche JM, Murugaraj R, Lee YS. 2010. Electrical and magnetic behaviour of nano structured Mg Fe_2O_4 spinel ferrite. *J Alloys Compd* 504(2): 395-402. doi: 10.1016/j.jallcom.2010.05.125

13. Afzal AB, Akhtar MJ, Nadeemm, Hassan MM. 2010. Dielectric and impedance studies of DBSA doped polyaniline/PVC composites. *Curr Appl Phys* 10(2): 601-606. doi: 10.1016/j.cap.2009.08.004

14. Gabal MA, Abdel-Daiem AM, Al Angari YM, Ismail IM. 2013. Influence of Al-substitution on structural, electrical and magnetic properties of Mn-Zn ferrites nanopowders prepared via the sol-gel auto-combustion method. *Polyhedron* 57: 105-111. doi: 10.1016/j.poly.2013.04.027

15. El-Sayed AM. 2002. Influence of zinc content on some properties of Ni-Zn ferrites. *Ceram Int* 28(4): 363-367. doi: 10.1016/S0272-8842(01)00103-1

16. Raghavender AT, Biliskov N, Skoko Z. 2011. XRD and IR analysis of nanocrystalline Ni-Zn ferrite synthesized by the sol-gel method. *Mater Lett* 65(4): 677-680. doi: 10.1016/j.matlet.2010.11.071

17. Shahane GS, Kumar A, Arora M, Pant RP, Lal K. 2010. Synthesis and characterization of Ni–Zn ferrite nanoparticles. *J Magn Magn Mater* 322(8): 1015–1019.

18. Gul IH, Ahmed W, Maqsood A. 2008. Electrical and magnetic characterization of nanocrystalline Ni-Zn ferrite synthesis by co-precipitation route. *J Magn Magn Mater* 320(3-4): 270-275. doi: 10.1016/j.jmmm.2007.05.032

19. Sharma R, Singhal S. 2013. Structural, magnetic and electrical properties of zinc doped nickel ferrite and their application in photo catalytic degradation of methylene blue. *Physica B Condens Matter* 414: 83-90. doi: 10.1016/j.physb.2013.01.015

20. Krishna KR, Kumar KV, Ravinder D. 2012. Structural and electrical conductivity studies in Nickel-Zinc ferrite. *Advances in Materials Physics and Chemistry* 2(3): 185-191. doi: 10.4236/ampc.2012.23028

21. Waldron RD. 1955. Infrared spectra of ferrites. *Phys Rev* 99(6): 1727-1735. doi: 10.1103/PhysRev.99.1727

22. Mallapur MM, Shaikh PA, Kambale RC, Jamadar HV, Mahamuni PU, et al. 2009. Structural and electrical properties of nanocrystalline cobalt substituted nickel zinc ferrite. *J Alloys Compd* 479(1-2): 797-802.doi: 10.1016/j.jallcom.2009.01.142

23. Kambale RC, Song KM, Koo YS, Hur N. 2011. Low temperature synthesis of nanocrystalline Dy^{3+} doped cobalt ferrite: structural and magnetic properties. *J Appl Phys* 110(5): 053910-053917. doi: 10.1063/1.3632987

24. Gabal MA, Al Angari YM. 2010. Low-temperature synthesis of nanocrystalline NiCuZn ferrite and the effect of Cr substitution on its electrical properties. *J Magn Magn Mater* 322(20): 3159-3165. doi: 10.1016/j.jmmm.2010.05.054

25. Zahi S. 2010. Synthesis, permeability and microstructure of the optimal Nickel-Zinc ferrites by sol-gel route. *Journal of Electromagnetic Analysis & Applications* 2(1): 56-62. doi: 10.4236/jemaa.2010.21009

26. Pathak TK, Vasoya NH, Lakhani VK, Modi KB. 2010. Structural and magnetic phase evolution study on needle-shaped nanoparticles of magnesium ferrite. *Ceram Int* 36(1): 275-281. doi: 10.1016/j.ceramint.2009.07.023

27. Wagner KW. 1913. The theory of imperfect dielectrics. *Ann Phys* 345(5): 817-855. doi: 10.1002/andp.19133450502

28. Mahalakshmi S, Manj KS. 2008. AC electrical conductivity and dielectric behavior of nano phase nickel ferrites. *J Alloys Compd* 457(1-2): 522-525. doi: 10.1016/j.jallcom.2007.03.045

29. Mohamed RM, Rashad MM, Haraz FA, Sigmund W. 2010. Structure and magnetic properties of nanocrystalline cobalt ferrite powders synthesized using organic acid precursor method. *J Magn Magn Mater* 322(14): 2058-2064.doi: 10.1016/j.jmmm.2010.01.034

30. Maxwell JC. 1929. Electricity and Magnetism, Vol.1. Oxford University Press, Oxford, Section 328.

31. Koops CG. 1951. On the dispersion of resistivity and dielectric constant of some semiconductors at audio frequencies. *Phys Rev* 83: 121. doi: 10.1103/PhysRev.83.121

32. Ravinder D, Reddy PVB. 2003. High-frequency dielectric behaviour of Li-Mg ferrites. *Material Letters* 57(26-27): 4344-4350. doi: 10.1016/S0167-577X(03)00093-4

33. Rezlescu N, Rezlescu E. 1974. Abnormal dielectric behaviour of copper containing ferrites. *Solid State Commun* 14(1): 69-72. doi: 10.1016/0038-1098(74)90234-8

34. Murthy VR, Sobbhandari J. 1976. Dielectric properties of some Ni-Zn ferrites at radio frequency. *Phys Status Solidi A* 36(2): 133-135. doi: 10.1002/pssa.2210360247

35. Olofa SA. 1994. Oscillographic study of the dielectric polarization of Cu-doped Ni-Zn ferrite. *J Magn Magn Mater* 131(1-2): 103-106. doi: 10.1016/0304-8853(94)90016-7

36. Thakura A, Mathura P, Singh M. 2007. Study of dielectric behaviour of Mn-Zn nano ferrites. *J Phys Chem Solids* 68(3): 378-381. doi: 10.1016/j.jpcs.2006.11.028

37. Kharabe RG, Devan RS, Kanamadi CM, Chougule BK. 2006. Dielectric properties of mixed Li-Ni-Cd ferrites. *Smart Mater Struct* 15(2): 36-39. doi: 10.1088/0964-1726/15/2/N02

38. Mohammed KA, Al-Rawas AD, Gismelseed AM, Sellai A, Widatallah HM, et al. 2012. Infrared and structural studies of $Mg_{1-x}Zn_xFe_2O_4$ ferrites. *Physica B Condens Matter* 407(4): 795-804. doi: 10.1016/j.physb.2011.12.097

39. Gabal MA, Al Angari YM, Zaki HM. 2014. Structural, magnetic and electrical characterization of Mg-Ni nano-crystalline ferrites prepared through egg-white precursor. *J Magn Magn Mater* 363: 6-12. doi: 10.1016/j.jmmm.2014.03.007

40. Hankare PP, Sankpal UB, Patil RP, Jadhav AV, Garadkar KM, et al. 2011. Magnetic and dielectric studies of nanocrystalline zinc substituted Cu-Mn ferrites. *J Magn Magn Mater* 323(5): 389-393. doi: 10.1016/j.jmmm.2010.08.050

41. Pervaiz E, Gul IH. 2014. High frequency AC response, DC resistivity and magnetic studies of holmium substituted Ni-ferrite: A novel electromagnetic material. *J Magn Magn Mater* 349: 27-34. doi: 10.1016/j.jmmm.2013.08.011

42. Lv L, Zhou JP, Liu Q, Zhu G, Chen XZ, et al. 2011. Grain size effect on the dielectric and magnetic properties of Ni Fe_2O_4 ceramics. *Physica E Low Dimens Syst Nanostruct* 43(10): 1798-1803. doi: 10.1016/j.physe.2011.06.014

43. Ata-Allah SS, Fayek MK. 2000. Effect of Cu substitution on conductivity of Ni-Al ferrite. *J Phys Chem Solids* 61(9): 1529-1534. doi: 10.1016/S0022-3697(00)00010-X

44. Iwauchi K. 1971. Dielectric properties of fine particles of Fe_3O_4 and some ferrites. *Japanese J Appl Phys* 10(11): 1520-1528. doi: 10.1143/JJAP.10.1520

45. Ata-Allah SS. 2004. XRD and Mossbauer studies of crystallographic and magnetic transformations in synthesized Zn-substituted Cu-Ga-Fe compound. *J Solid State Chem* 177(12): 4443-4450. doi: 10.1016/j.jssc.2004.09.021

46. Mangalaraja RV, Kumar AS, Manohar P, Gnanam FD. 2002. Magnetic, electrical and dielectric behaviour of $Ni_{0.8}Zn_{0.2}Fe_2O_4$ prepared through flash combustion technique. *J Magn Magn Mater* 253(1-2): 56-64. doi: 10.1016/S0304-8853(02)00413-4

47. Patil DR, Chougule SS, Lokare SA, Chougule BK. 2008. Electrical properties of $xNiFe_2O_4$ + (1– x) $Ba_{0.7}Sr_{0.3}TiO_3$ composites. *J Alloys Compd* 452(2): 414-418. doi: 10.1016/j.jallcom.2006.11.021

48. Ajmal M, Maqsood A. 2007. Influence of zinc substitution on structural and electrical properties of $Ni_{1-x}Zn_xFe_2O_4$ ferrites. *Materials Science and Engineering B* 139(2-3): 164-170.

49. Goldman A. 1990. Modern ferrites technology. Van Nostrand Reinhold, New York, USA.

50. Patange SM, Shirsath SE, Lohar KS, Jadhav SS, Kulkarni N, et al. 2011. Electrical and switching properties of $NiAl_xFe_{2-x}O_4$ ferrites synthesized by chemical method. *Physica B Condens Matter* 406(3): 663-668.

51. Hankare PP, Sankpal UB, Patil RP, Mulla IS, Sasikala R, et al. 2010. Synthesis and characterization of nanocrystalline zinc substituted nickel ferrites. *J Alloys Compd* 496(1): 256-260. doi: 10.1016/j.jallcom.2010.01.009

52. Fradin FKY. 1985. Treatise on magnetic materials: science and technology, 25 Academic Press, New York, USA.